The 2009 IEEE/RSJ International Conference on
Intelligent Robots and Systems
October 11-15, 2009 St. Louis, USA

# A robotic closed-loop scheme to model human postural coordination

Vincent Bonnet, Philippe Fraisse, Nacim Ramdani, Julien Lagarde, Sofiane Ramdani, Benoit G. Bardy

*Abstract*— **This paper models recent data in the field of postural coordination showing the existence of self-organized postural states, and transition between them, underlying supra-postural tracking movements. The proposed closed-loop controller captures the complex postural behaviors observed in humans and can be used to implement efficient and simple balance control principles in humanoids.**

*Index Terms*— **postural coordination, redundant tracking task, bio-inspired balance controller**

## I. Introduction

Due to their anthropomorphic structure, humanoid robots often present dynamic similarities with humans. Hence the fields of humanoid robotics and of human movement science can inspire each other.

In 1985, Nasher and Mc Collum [1] observed two postural *strategies* at the muscular activation level, when the whole upright body reacts to an external perturbation: The *ankle* strategy which is characterized by a large activity of the ankles and the *hip* strategy which corresponds to the coordinative activation of the hips and the ankles. These postural strategies have inspired the development of a bio-inspired balance controller allowing a humanoid robot to recover from large disturbances and still maintain an upright posture [2], [3]. In the motor control field, Kuo [4] developed a double inverted pendulum (DIP) model with feasible acceleration set (FAS) and an optimal control law weighting excursion of the center of mass and deviations from the upright position. Using the FAS framework, Park [5] optimized joint feedback gains to fit human data for different kind of perturbations and showed that trajectories of joint angles and joint torques were scaled with perturbation magnitude and conform with the postural strategy observations.

Using a parametric experimental paradigm, Bardy *et al* demonstrated the dynamical properties of the joint coordination in the sagittal plane [6]. Bardy *et al* described the pattern of coordination between the ankle and the hip joints using a single collective variable, the *relative phase* between the ankle and the hip. They had standing participants moving back and forth in the sagittal plane in order to track the displacement of a virtual target. In agreement with the coordination dynamics framework [7], this key parametric manipulation revealed the fundamental non linear properties of the postural system, such as phase transition, multistability, critical fluctuations, hysteresis, and critical slowing down. In particular, two coordination modes between ankle and hip were observed, which were preferentially exhibited depending on the target's frequency: *In-phase* mode at low frequencies and *anti-phase* mode for high frequencies.

Martin *et al.* [8] used a constrained optimization process to analyze Bardy *et al*. 's results, and showed that the location of the center of pressure (CoP) can drive the selective of the coordination mode.

In a previous work [9], we studied in more details Bardy *et al*.'s with a method similar to the one used in [8] and implemented the obtained coordination modes in the HOAP-3 and HRP2 humanoid robots. We showed that the in-phase mode corresponds to the minimum energy mode for low frequencies and that the anti-phase mode is the only one able to maintain balance for high frequencies. In our simulations, the anti-phase mode was selected when the CoP reached the base of support (BoS) limits. This result may be used to improve the balance control in humanoid robots.

However, the approach described above considers only steady state behaviors and thus is not capable of capturing the transient dynamics observed during human postural behaviors such as the hysteresis phenomenon for instance. Non-linear coupled oscillators are classically used to model these human dynamical coupling phenomena [10]. However, these ocillators involve several unknown parameters which have to be identified and whose connection with the actual system is difficult to delineate.

The goal of this paper is to propose a non-linear closed-loop model of the supra-postural behavior documented by Bardy, which is composed of a DIP as biomechanical model, a classical controller proportionnal-derivative and an adaptive ankle torque saturation to ensure balance. The ability to reproduce the biological couplings, in a dynamical task, should ameliorate or simplify balance control in humanoids.

## II. Human experimentation

The aim of the experiment is to provide a database of human behavior against which the results of simulation reported in section IV can be compared.

### A. Methods

Following up previous studies [11], [12], the experimental paradigm employed a task consisting in tracking with the

V. Bonnet, P. Fraisse and N. Ramdani are with the LIRMM UMR 5506 CNRS, Univ. Montpellier 2, 161 rue Ada, Montpellier, 34392 France.

N. Ramdani is with the Constraints Solving, Optimization, Robust Interval Analysis (COPRIN) Project, Institut National de Recherche en Informatique et en Automatique (INRIA) Sophia-Antipolis, Nice FR-06902, France.

J. Lagarde, S. Ramdani and B. G. Bardy are with the EDM EA 2991, Univ. Montpellier 1, EDM, 700 av. du pic Saint Loup, Montpellier, 34090 France.

B. G. Bardy is with Institut Universitaire de France, 103 Bd St Michel, Paris, 75005 France

head a target moving while standing. Participants stood on a force platform in front of a physical target moved by a linear motor, with the knees locked and the soles in contact with the ground (Fig. 1).The experiment was performed on 11 healthy male subjects, with mean age 25, mean weight 75kg and mean size 1.79m. The displacement of the target was sinusoidal with 10cm amplitude, the frequency was increased from 0.1Hz to 0.65Hz by 0.05Hz steps and during 10 periods. A motion captude system was used to estimate the joint positions, with 8 cameras tracking 15 relfective markers placed on the right side of the subject.

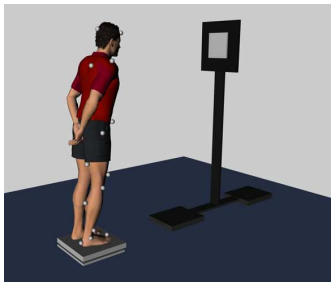

Fig. 1. Experimental device. Physical target moved by a linear motor, force plate and motion capture device.

### B. Experimental results

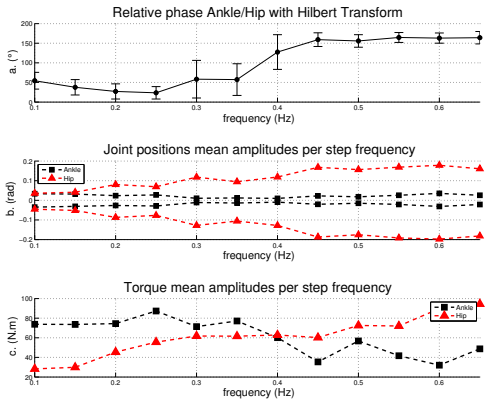


Fig. 2. Typical human experimental results. (a) Ankle/hip relative phase, showing a transition frequency around 0.4Hz (b) Peak to peak joint positions. Each point is the mean value of the maximum (or minimum) joint position reached during the 10 oscillations performed at each frequency step. Hip position is larger than the ankle position. (c) Estimation of joint torque amplitudes. Ankle torque is larger for in-phase mode and inversely for anti-phase mode

Fig.2 shows results for a typical subject (75kg, 1.80m).

On (Fig. 2a), the mean values of the (Hilbert-transformed) relative phase between ankle and hip positions are represented as a function of the frequency step. The depicted error bars correspond to the standard deviations during the 10 oscillations achieved at each frequency step. A transition is observed from in-phase to anti-phase mode around 0.4Hz.

Joint positions are presented on Fig. 2b by minima and maxima values. Each point is the mean value of the maximum (or minimum) joint position reached during the 10 oscillation periods performed at each frequency step. For the in-phase mode, i.e., at low frequencies, the joint positions amplitude difference are small, with large individual differences in terms of joint amplitude. The hip amplitude is larger than the ankle amplitude for the anti-phase mode as mentioned in [12].

Fig. 2(c) depicts mean values for torque amplitude estimation at each frequency step. Torque values were estimated by using the inverse dynamical model of the DIP. They indicate a larger ankle torque amplitude for in-phase mode and a larger hip torque amplitude for anti-phase in agreement with the ankle and hip strategy reported in [1] and by Runge *et al.* [13]

These observations were observed for all participants and are in accordance with [11], [6], even though the actual transition frequency and joint amplitudes depend on the specific subject body type.

## III. Modeling Postural Behavior

### A. Biomechanical model

Barin [14] shows the relevance of a inverted pendulum structure in the case of a human sagittal plane task. In addition, the Bardy's paradigm focussed on the hip and ankle joints, so a DIP in the sagittal plane is used as a biomechanical model (Fig. 3). In the task space we only set the horizontal head position, so the actuated system is redundant with respect to the task.

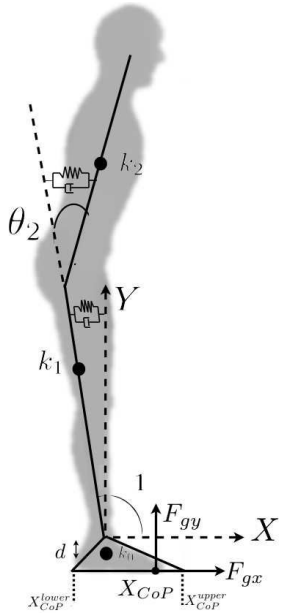


Fig. 3. Double inverted pendulum used to model postural coordination. Spring damping system are added at each joint to represent passive and reflex muscle influences.

Balance is described by the position of the CoP within the BoS, which can be expressed as a function of the dynamic parameters (eq.1).

$$X_{CoP} = \frac{(\Gamma_1 - F_{gx}d + m_0 k_0 g)}{F_{gy}} \quad (1)$$

where $F_{gx}$ is the horizontal ground reaction force, $F_{gy}$ the vertical one, $\Gamma_1$ the ankle torque, and $m_0$ and $k_0$ foot parameters. Euler's equations were used for the calculation of the ground reaction forces.

### B. Closed-loop modeling

In the robotics field, many control schemes exist for redundant applications. Whitin the framework of the operational space formulation defined by [15], Sentis [16] proposed a task-posture decoupling for humanoids. This controller enables humanoids to execute tasks in operational space and, at the same time, to control the CoP location.

Inspired by classical work on postural strategies, a decoupled controller with a specific control on the CoP location was proposed by [3]. We accept that the instantaneous control of the CoP is necessary in many applications, but in the case of Bardy's paradigm, we focussed only on the human observations. In the human motor-control literature, there are no obvious evidences that the CoP location is directly controlled by the CNS. In addition [8], [9] emphasized the fact that human postural system changes its coordination mode when the CoP reaches the BoS limit.

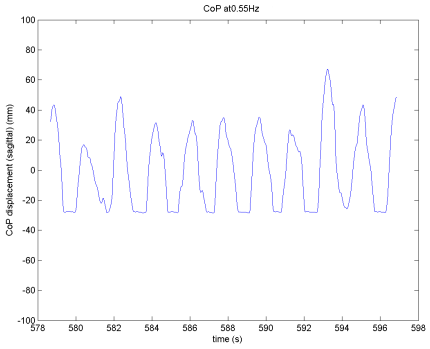


Fig. 4. Typical CoP displacement for one step frequency (0.55Hz). The CoP location is bound by lower BoS limit.

Fig. 4 presents a typical CoP trajectory for one frequency step, during the experiment with humans. It is clear that the CoP location is saturated due to the BoS and a limitation of the human ankle torque. The following control scheme takes into account these observations with a non-linear closed-loop modeling, which is composed of a double inverted pendulum as biomechanical model, a classical controller in operational space, and an adaptive torque saturation to ensure robot's balance.

On Fig. 5, $DKM$ is the direct kinematics model, $K_{pj}$ and $K_{dj}$ are the proportional and derivative controller gains in the joint space, $J^+$ is the pseudoinverse matrix and $\Gamma_{1Sat}$ the adaptive ankle saturation.

It is well attested that the use of the pseudoinverse matrix in kinematics redundant problems minimizes the norm of

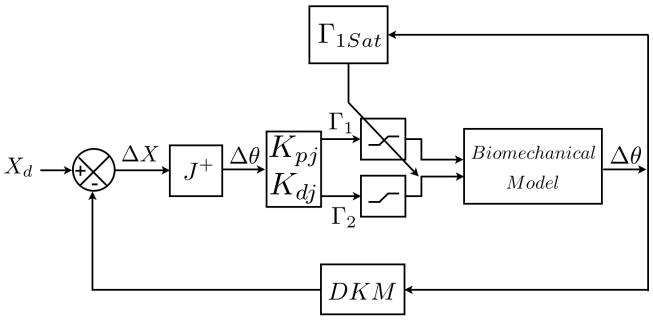


Fig. 5. Block diagram of postural coordination controller

the velocity vector $||\dot{\theta}||^2$ at a given time. By analogy with inverse kinematics, the pseudoinverse matrix used in the control scheme depicted on Fig. 5 minimizes the norm of the torque vector $||\Gamma(t)||^2$.

To complete the modeling, the issue of maintaining the CoP inside the BoS needs to be addressed. Since the CoP is a function of the ankle torque (see eq. 1), we propose to use an adaptive torque saturation for the ankle. Note that the use of the saturation loop does not imply the control of instantaneous CoP location. At each time step, the thresholds for ankle torque saturation maintaining the CoP inside the BoS limits were computed. In the following equations, the upper threshold for torque saturation is given by

$$\Gamma_{1Sat}^{upper} = F_{gx}d - m_0 k_0 g + X_{CoP}^{upper} F_{gy} \quad (2)$$

where $X_{CoP}^{upper}$ is the upper BoS bound, $m_0$ and $k_0$ are foot parameters, and the lower one is given by

$$\Gamma_{1Sat}^{lower} = F_{gx}d - m_0 k_0 g + X_{CoP}^{lower} F_{gy} \quad (3)$$

where $X_{CoP}^{lower}$ is the lower BoS bound.

Finally, if at a given time previous step, $\Gamma_1$ is saturated then the postural system acts mainly on hip torque in order to execute the task.

### C. Consideration of the human joint properties

In humans, the net joint torques are produced by muscle contractions and by muscle viscoelastic passive properties. Muscle activation, which controls the level of muscle contraction (i.e. muscle stiffness), is due to a direct control of the central nervous system (CNS) and to the reflex loops. The spindle sensors provide feedback on muscle length and velocity, which enable the reflex loops to keep the muscle length at a value corresponding to its rest position as mentioned by Van der Helm in [17].

It's well attested that spindle reflexes are important in postural muscles, especially in terms of stiffness control and disturbance rejection. Fitzpatrick [18] has linked a part of the joint stiffness with the feedback reflex gain, by studying small perturbations on quiet standing and by manipulating the availability of sensory feedback.

So a simplified representation of human joints is used by adding passive spring damping systems at each joint.

Currently, the stiffness and the viscous coefficient friction of joints are kept constant for all frequency steps. However in the next section IV-A preliminary fitting results on human data, by tuning these stiffnesses and viscosities by frequency step, will be presented.

## IV. Fit between model and human data

The simulation results obtained with the closed-loop controller are presented in this section. Simulation parameters are given for the same typical subject and the same frequency evolution described in section II. The length of the foot is 20cm. The controller's gains and passive spring damping coefficient are constant during the simulation.

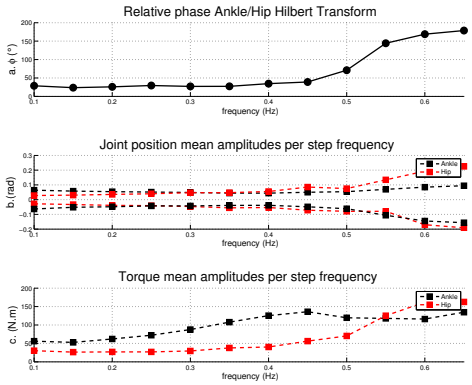


Fig. 6. Typical simulation results. (a) Ankle/hip relative phase showing a transition frequency around 0.5Hz (b) Peak-to-peak joint positions. Each point is the mean maximum/minimum value of 10 oscillation periods at a frequency step. Hip position is larger than ankle position for anti-phase, and conversely for in-phase mode (c) Joint torque amplitudes. Ankle torque is larger for in-phase mode and hip torque is larger for anti-phase mode

On Fig. 6a, one can see two distinctive coordination modes similar to the ones exhibited in humans (see section II). The in-phase mode appears at low frequencies and the anti-phase mode appears at high frequencies. Note however that the transition between them occurs around 0.5Hz in our simulation whereas it occurred around 0.4Hz in the human experiments.

This discrepancy may be induced by the approximate nature of the model used.

Fig. 6b shows that at low frequencies, the joint positions have similar amplitudes. This result is fairly close to the one observed with humans (see Fig 2b). At high frequencies, simulation results show a larger motion for the hip than for ankle position as observed in the human data.

Considering now the joint torque amplitudes (Fig. 6b), the ankle torque is larger than the hip torque for in-phase mode, and conversely for anti-phase mode, in accordance with the human observations.

One can see that our closed-loop model is able to reproduce the human postural observations. An optimization process to tune the gains of the closed-loop system would bring more precision for the human data fitting.

### A. *Effect of joint flexibility*

In this section, we present a method to compute the proportional and derivative gains of the controller including the passive spring-damping parameters for each frequency step. The simulation data resulting from the computation method are then compared with the experimental ones (see Fig. 2).

The calculation of these parameters is based on an optimization process using (eq. 4) as a cost function and the physiological limitation as a constraint.

$$J = \sum_{t=0}^{10T} \left( \sum_{i=1}^{2} (\theta_{i_{hum}} - \theta_{i_{sim}})^2 \right) \quad (4)$$

$T$ is the period of the signal for a given frequency, $\theta_{hum}$ and $\theta_{sim}$ are respectively the human experimental and simulation output joint positions.

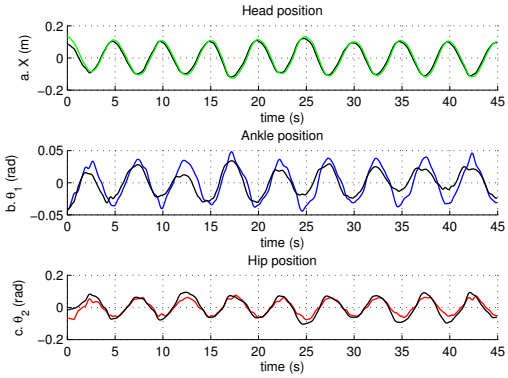


Fig. 7. Optimization results for in-phase mode at 0.2Hz. Human joint positions (black) and simulation results (color) for optimized model coefficients.

Fig. 7, 8 and 9 show the human movement of the head, ankle and hip joints and the ones computed with the optimization process (eq. 4). The first optimization results for in-phase and anti-phase modes and during the phase transition are similar to those measured experimentally on human being, validating in this way the model (see Fig. 7, 8 and 9).

The introduction of stiffness coefficients into the model derives simulation results which are closer to actual ones, than the ones obtained with a rigid model. Furthermore the discrepancy between actual data and simulation results can be significantly reduced if the stiffness coefficients values are tuned at each frequency level. Indeed, this tuning process is equivalent to adjusting as close as possible the dynamical behavior of each movement at a given frequency. As regarding physiological meanings, stiffness parameter adaptation can be connected to the different muscle activation levels needed to achieve movement. Currently, the relationships between the gains $K_{pj}$, $K_{dj}$, and the spring-damping parameters and the evolution of their values with the frequency steps have to be analyzed. In fact, we observe a strong coupling between these parameters that could be induced by a non linear function such as a muscle model because the optimal values

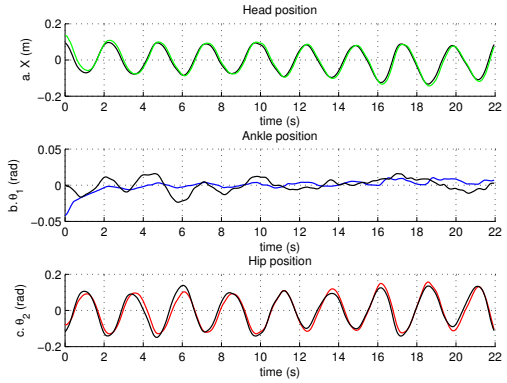


Fig. 8. Optimization results around transition frequency at 0.4Hz. Human joint positions (black) and simulation results (color) for optimized model coefficients.

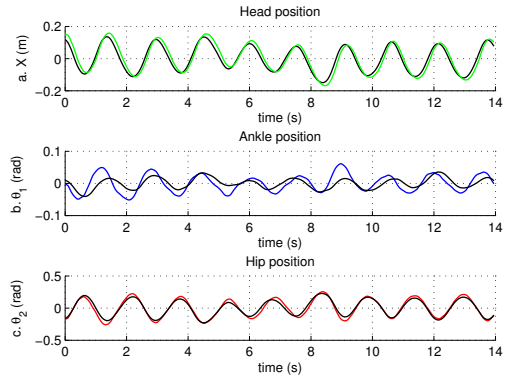


Fig. 9. Optimization results for anti-phase mode at 0.65Hz. Human joint positions (black) and with simulation results (color) for optimized model coefficients.

obtained for the coefficients depend on the subject for a given frequency.

Nevertheless, the main goal of this section was to show that adding variable stiffness and viscosity parameters significantly improve modelling. Indeed, we are now convinced that adding muscle models should improve model accuracy because they correspond to a varying active stiffness depending on joint angle and angular velocity. This will be the next step of our work. Besides, adding stiffness in the lower limbs of anthropomorphic structures increases movement efficiency and reduces energy consumption. This could be a relevant research for the mechanical design of humanoid robot.

## V. Analysis of the Tracking Task

### A. Relative phase transition analysis

In order to further analyze the behavior of the closed-loop scheme, the target frequency was up-chirped from 0.1Hz to 1Hz in simulation. The subject parameters was the same typical as in section II. Two cases are considered here: the adaptive torque saturation is activated ( Fig. 10) and then is disabled (Fig.12).

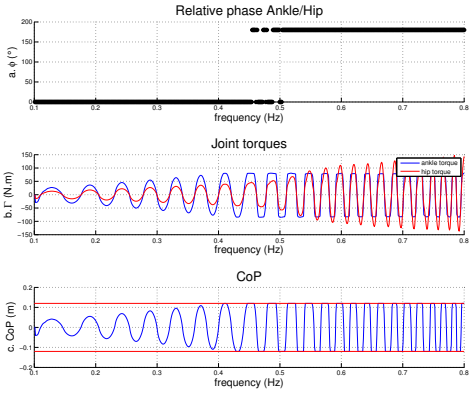


Fig. 10. Ankle/hip relative phase (a), joint torque (b) and CoP motion (c). Transition frequency occurs at 0.5Hz when the adaptive ankle saturation is activated. Hip torque is larger than ankle torque for the anti-phase mode. The CoP constraint is able to guide the coordination mode.

Fig. 10 shows the Hilbert relative phase on the simulation results, the joint torques and the CoP location. We can see that the CoP stays inside the BoS limits (Fig. 10c) and that when it reaches these limits the coordination mode suddenly changes from in-phase to anti-phase mode (Fig. 10a). This is in agreement with previous works [9], where we show on humanoid robots (see Fig. 11) that the anti-phase mode is the stablest mode.

(a) t=0 sec (b) t=0,75 sec (c) t=1.45 sec

Fig. 11. HOAP3 experiments with in-phase coefficients at high frequency ($f = 1$Hz, $BoS = 1$cm, $A_t = 5$cm). The robot cannot maintain its balance and falls backward.

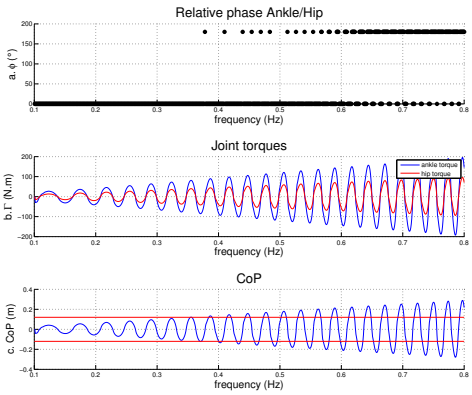


Fig. 12. Ankle/hip relative phase (a), joint torque (b) and CoP motion (c). Transition frequency occurs around 0.6Hz when the adaptive ankle saturation is activated. Hip torque is larger than ankle torque for the anti-phase mode. The CoP constraint is able to guide the coordination mode.

On Fig. 12, one can see that a change in the coordination mode occurs even when the CoP constraint is disabled, but at a higher frequency (0.6Hz) compared to Fig. 10 where the CoP constraint is activated. In fact, since the pseudoinverse matrix, in the closed-loop scheme, minimizes $||\Gamma(t)||^2$ the system reaches the minimal energy solution. So in human the phase transition emerges from both equilibrium constraint and energy minimization.

### B. Hysteresis phenomenon

An hysteresis phenomenon, hallmark of non linear systems, has been observed in human experiments [11]. In the postural coordination framework, the hysteresis phenomenon has never been modeled. The closed loop modeling introduced in this article exhibits such an hysteresis phenomenon when the target frequency is up-chirped and then down-chirped (Fig. 13). Note that the gain values of the controller and the dynamics of the reference target influence the hysteresis region. Current work now examines the energetic cost for different types of reference dynamics around the transition frequency in order to better understand the hysteresis phenomenon.

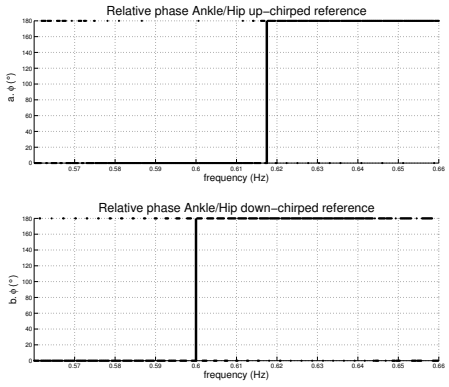


Fig. 13. Typical simulation hysteresis phenomena. (a) The relative phase for up-chirped reference signal. (b) The relative phase for down-chirped reference signal.

## VI. Conclusions

The closed-loop controller model we have developed, provides realistic predictions of postural sway movements during head tracking task and offers a better comprehension of the postural coordination phenomena. The computed results are consistent with human observations related to similar experimental paradigms. Many of the differences between experimental and simulated results can be attributed to simplifications in the modeling and could be reduced by adding an active and variable joint stiffness, using a non linear muscle model with reflex loops.

The results obtained when varying simulation parameters, show that the sudden bifurcation emerges from both equilibrium constraint and cost minimization.

The closed-loop modeling also allows to reproduce the hysteresis phenomenon observed in human experiments.

By now, we believe that our model of postural coordination is promising in capturing behavioral invariants observed in human. In addition, our approach allows to isolate and study the mechanical phenomenon involved in human coordinations, unlike the descriptive model presented by [10].

A similar framework used by [2] for decoupled control tasks are able to reproduce a wide range of adaptive behaviors. That the reasons why we believe they are appropriate for humanoid robotics. The closed-loop controller is currently under development on humanoid robots HOAP-3, even if a low-level adaptation is necessary since we use a torque control vector while most humanoids are controlled in position via a local regulator.

The disturbance rejection properties of our controller are being characterized. This controller will be able to automatically change the phase difference and the joint amplitude necessary to maintain balance.

## References


[1] L. Nashner and G. McCollum, "The organization of postural movements: a formal basis ansd experimental synthesis," *Behavioral and Brain Sciences*, vol. 26, pp. 135–172, 1985.

[2] B. Stephens, "Humanoid push recovery," *IEEE Int. Conf. on Humanoid Robots*, 2007.

[3] B. . Stephens, "Integral control of humanoid balance," *IROS'07*, 2007.

[4] A. Kuo, "An optimal control model for analyzing human postural balance." *IEEE Trans. Biomed. Eng.*, vol. 42, pp. 87–101, 1995.

[5] S. Park, F. Horak, and A. Kuo, "Postural feedback responses scale with biomechanical constraints in human standing," *Exp Brain Res*, vol. 154, no. 417-427, 2004.

[6] B. Bardy, O. Ouillier, R. Bootsma, and T. Stoffregen, "Dynamics of human postural transitions," *ExP. Psychol. Hum. Percept. Perform.*, vol. 28, pp. 499–514, 2002.

[7] J. Kelso, *Dynamics Patterns, The Self-Organization of brain and behavior*. The MIT Press, 1995.

[8] L. Martin, V. Cahouet, M. Ferry, and F. Fouque, "Optimization model predictions for postural coordination modes," *Journal of Biomechanics*, vol. 39, pp. 170–176, 2006.

[9] V. Bonnet, J. Lagarde, P. Fraisse, N. Ramdani, S. Ramdani, P. Poignet, and B. Bardy, "Modelling of the human postural coordination to improve the humanoids control of balance," *IEEE Int. Conf. on Humanoid Robots*, 2007.

[10] H. Haken, J. Kelso, and H. Bunz, "A theorical model of phase transitions in human hand movements," *Biological Cybernetics*, vol. 51, pp. 347–356, 1985.

[11] B. Bardy, L. Marin, T. Stoffregen, and R. Bootsma, "Postural coordination modes considered as emergent phenomena," *Exp. Psychol. Hum. Percept. Perform.*, vol. 25, pp. 1284–1301, 1999.

[12] O. Oullier, B. Bardy, T. Stroffregen, and R. Bootsma, "Postural coordination in looking and tracking tasks," *Human Movement Sciences*, vol. 21, pp. 147–167, 2002.

[13] C. Runge, C. Shupert, F. Horak, and F. Zajac, "Ankle and hip postural strategies defined by joint torques," *Gait and Posture*, vol. 10, pp. 161–170, 1999.

[14] K. Barin, "Evaluation of a generalized model of human postural dynamics and control in the sagittal plane," *Biological Cybernetics*, vol. 61, pp. 37–50, 1989.

[15] O. Khatib, "A unified approach for motion and force control of robot manipulators: The operational space formulation," *IEEE Journal of Robotics and Automation*, vol. 3, no. 1, pp. 43–53, 1987.

[16] L. Sentis, "Synthesis and control of whole-body behaviors in humanoid systems," Ph.D. dissertation, Stanford University, 2007.

[17] J. M. Winters and P. E. Crago, *Biomechanics and Neural Biomechanics and Neural Control of Posture and Movement*, Springer-Verlag, Ed., 2000.

[18] R. Fitzpatrick, R. Gorman, D. Burke, and S. Gandevia, "Postural proprioceptive reflexes in standing human subjects: bandwidth of response and transmission characteristics," *Journal of Physiology*, vol. 458, pp. 69–83, 1992.